ISJ 12: 46-65, 2015 ISSN 1824-307X

RESEARCH REPORT

Nitric oxide production in celomocytes of the earthworm *Eisenia hortensis* following bacterial challenge

SR Cook, MM Sperratore, SL Fuller-Espie

Science Department, Cabrini College, 610 King of Prussia Road, Radnor, Pennsylvania 19087-3698, USA

Accepted February 6, 2015

Abstract

In this *in vitro* investigation, nitric oxide (NO) production was induced within celomocytes of the earthworm *Eisenia hortensis* following microbial challenge. Celomocytes were pre-loaded with the fluorescent indicator 4-amino-5-methylamino-2', 7'-difluorofluorescein diacetate (DAF-FM DA) in order to detect the presence of intracellular nitric oxide subsequent to a 16 h incubation with chemically-fixed soil bacteria including *Bacillus megaterium, Arthrobacter globiformis, Pseudomonas stutzeri,* and *Azotobacter chroococcum* at a range of multiplicities of infection (MOIs). Flow cytometric analysis measuring increases in relative fluorescence intensity (RFI), which is directly proportional to the amount of intracellular NO produced, permitted determination of statistical significance ($p < 0.05$) of exposed celomocytes compared to baseline controls. Significant increases in NO were detected reproducibly in celomocytes treated with all bacterial species used. The most prominent results were observed after exposure to Gram positive *B. megaterium* and *A. globiformis* where 100 % of earthworms tested exhibited statistically significant increases of RFI at MOIs of 100:1 and 500:1, respectively. Furthermore, significant decreases in NO production in bacteria-stimulated earthworm celomocytes incubated with the NOS inhibitor aminoguanidine hydrochloride were observed. These results demonstrate microbial induction of NO synthesis in earthworms and provide evidence of an antimicrobial role of NO in the innate immune system.

Key Words: nitric oxide; earthworm; celomocytes; aminoguanidine; flow cytometry; DAF-FM DA

Introduction

Invertebrates rely solely on the non-specific defense mechanisms employed in the innate immune system in order to combat potentially infectious microorganisms, unlike vertebrates, which possess both innate and adaptive immune systems. The induction of the innate immune response depends on the recognition of highly conserved features specific to microorganisms that are not present in the host. These extracellular structures or products of microbial metabolism, called pathogen- or microbe-associated molecular patterns (PAMPs or MAMPs), are recognized by receptors on the surface of phagocytic cells called pattern-recognition receptors (PRRs). PRRs function to initiate the process of phagocytosis and stimulate the expression of proteins that facilitate the destruction of the pathogen (Cooper, 2006). One group of PRRs includes the phagocytic receptors, which bind to the pathogen and aid in its uptake into the host immunocyte. Another group of PRRs are the signaling receptors, called Toll-like receptors (TLRs). Several different TLRs have been identified, and each recognizes a unique set of PAMPs. For example, TLR2 is able to recognize lipoteichoic acid (LTA) found in Gram-positive bacteria, and TLR4 is able to recognize lipopolysaccharide (LPS) in Gram-negative bacteria. The recognition of PAMPs by TLRs induces a signal transduction pathway which results in the transcription of genes encoding essential antimicrobial products that aid in the host organism's defense against infection and the killing of pathogenic microbes (Aderem and Ulevitch, 2000). First identified in the fruit fly *Drosophila* species, TLR homologues have been identified in both invertebrates and vertebrates, indicating that this system of pathogen recognition has been evolutionarily preserved (as reviewed by Takeda and Akira, 2001). Examples of invertebrate TLR homologues include TOL-1, found in the nematode *Caenorhabditis elegans* (Tenor and Aballay, 2008), and *Ea*TLR, found in the annelid *Eisenia andrei* (Škanta *et al.*, 2013).

Corresponding author:
Sheryl L. Fuller-Espie
Science Department
Cabrini College
610 King of Prussia Road, Radnor, PA 19087-3698, USA
E-mail: sfuller-espie@cabrini.edu

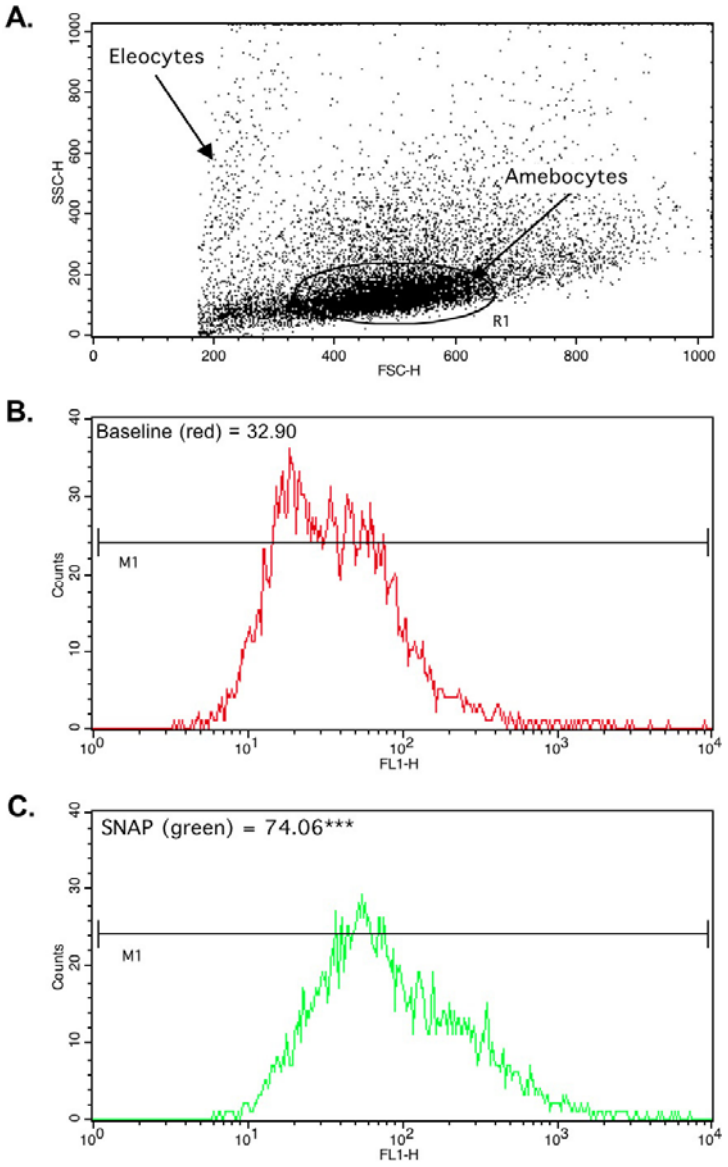

Fig. 1 Representative flow cytometric analysis set-up for NO and NOS inhibition assays measuring NO production in celomocytes labeled with the fluorescent indicator DAF-FM DA. (A) Dot plot of forward scatter (FSC) (abscissa) versus side scatter (SSC) (ordinate) of all events collected. A region (R1) was set around the amebocyte population to exclude bacteria (where possible), cellular debris, large cellular aggregates, and autofluorescent eleocytes in final analysis. (B) Histogram of the baseline control sample gated on R1 depicting the relative fluorescence intensity (RFI) measured by the FL-1 detector (abscissa) in log scale versus cell count (ordinate). The RFI values correlate with the concentration of NO in each cell. A marker (M1) was placed to facilitate the measurement of the geometric mean of RFI of the entire amebocyte population, as shown in the left corner of the histogram. (C) Histogram of the positive control sample (SNAP) gated on R1 depicting the RFI as described in B, with the geometric mean of RFI shown in the left corner of the histogram. Statistical analysis was performed on the geometric mean of RFI, and asterisks indicate statistically significant levels of NO production above baseline control, as determined by t-test: paired two sample for means (* = $p \leq 0.05$; ** = $p \leq 0.005$; and *** = $p \leq 0.0005$).

Previous studies in our lab have focused on the immune cell responses of the earthworm *Eisenia hortensis*, including phagocytosis and apoptosis (Fuller-Espie *et al.*, 2010), heat-induced stress response (Tumminello and Fuller-Espie, 2013), PAMP- and heavy metal-induced mitochondrial membrane depolarization (Bearoff and Fuller-Espie, 2011; Nacarelli and Fuller-Espie, 2011), and cytokine-mediated responses (Fuller-Espie *et al.*, 2008; Fuller-Espie, 2010). As part of the phylum Annelida, *E. hortensis* possess leukocyte-like cells, called celomocytes, which are located in the celomic cavity and function to carry out the immune responses against pathogenic microbes (Cooper *et*

al., 2002). Three main populations of celomocytes have been characterized into three different subpopulations, the chloragocytes (eleocytes), the hyaline amebocytes, and the granular amebocytes, which have different functional properties (Engelmann *et al.*, 2004). Both the hyaline and granular amebocytes participate in the immune responses of phagocytosis and encapsulation, where the eleocytes do not exert phagocytic activity, but play roles in nutrition, excretion, and the synthesis of cytotoxic and antibacterial molecules (Valembois *et al.*, 1985; Dales and Kalaç, 1992). In addition, the amebocytes have the capacity to synthesize free radicals with antimicrobial characteristics (Rivero, 2006; Valembois and Lasségues, 1995). Once a pathogenic microbe is recognized and engulfed by the host phagocyte, lysosomal enzymes begin to synthesize reactive oxygen intermediates (ROIs) and reactive nitrogen intermediates (RNIs), such as hydrogen peroxide and nitric oxide (NO), respectively. These metabolites are then able to react with oxygen and oxygen-related intermediates to ultimately form toxic species that have DNA-damaging and enzymatic properties (Rivero, 2006).

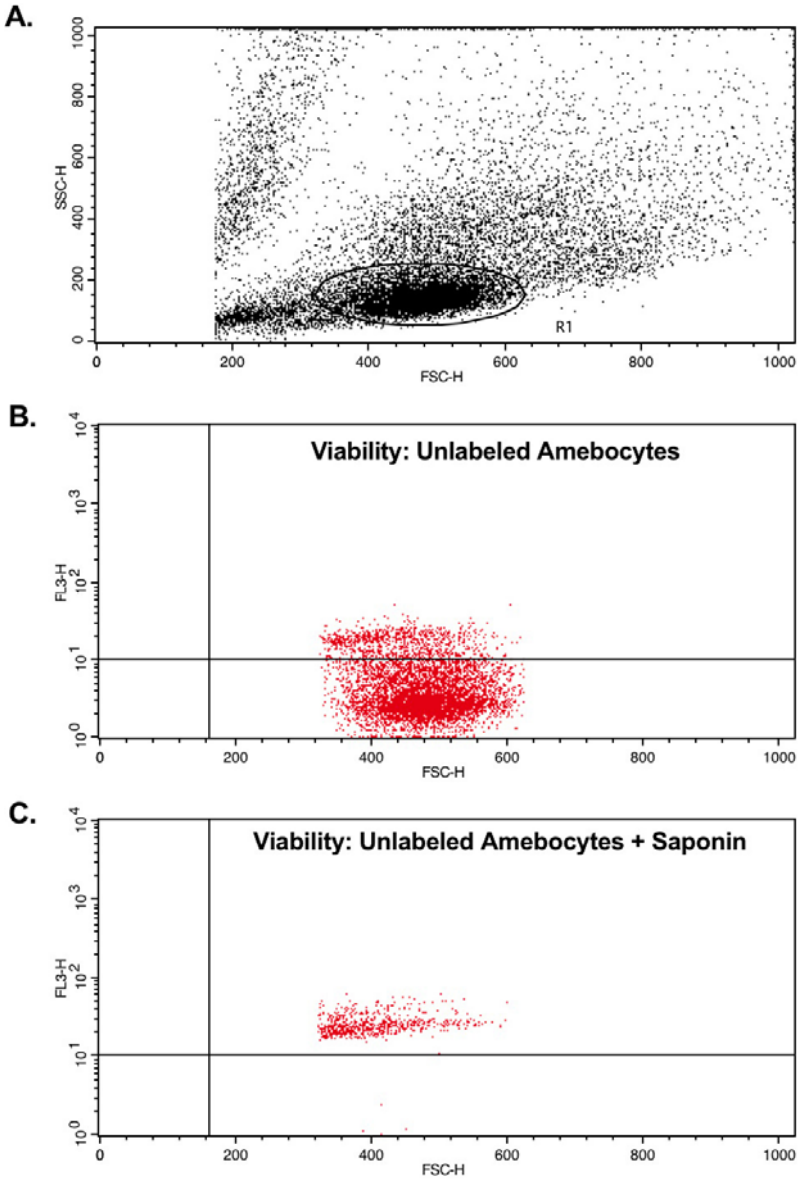

Fig. 2 Flow cytometric analysis set-up for measurement of viable unlabeled celomocytes after addition of 7-AAD. (A) Dot plot of FSC (abscissa) versus SSC (ordinate) is shown. A region (R1) was added as described in Figure 1. (B) Dot plot of FSC (abscissa) versus FL-3 (ordinate) in log scale, gated on R1, is shown. A quadrant marker was placed to facilitate the measurement of the percentage of viable cells after overnight incubation with relevant treatment. Shown here is media-treated celomocytes. Viable cells reside in the lower right quadrant, while non-viable cells reside in the upper right quadrant, where a much higher RFI is observed when saponin is added (C).

As reviewed by Rivero (2006), most of what we currently know about intracellular production of NO comes from studies on vertebrate organisms, where NO has been shown to play a role in a wide variety of physiological processes. This highly reactive, unstable gas is formed from the oxidative deamination of the amino acid L-arginine to citrulline, and is facilitated by the enzyme nitric oxide synthase (NOS) (Burgner *et al.*, 1999). To date, there are three isoforms of NOS that have been identified in different cellular populations. Although each isoform is able to catalyze the same reaction, they differ in respect to their regulation, amplitude and duration of NO production, and their cellular and tissue distribution (Bogdan, 2001). Constitutive NOS (cNOS) includes two isoforms, neuronal NOS (nNOS) and endothelial NOS (eNOS). They are continually expressed in neuronal tissue and vascular endothelial cells, respectively (as reviewed by Alderton *et al.*, 2001). The cNOS isoforms facilitate the production of NO at low levels, in which NO plays a role as a signaling molecule in processes such as neurotransmission and vascular regulation (as reviewed by Colasanti and Venturini, 1998). In contrast, the third isoform, inducible NOS (iNOS), is absent in resting cells, but is rapidly synthesized in immune-competent cells, such as macrophages and neutrophils, in response to cytokines and pro-inflammatory mediators (Martínez, 1995; Rivero, 2006). The synthesis of iNOS facilitates the production of NO at high levels, in which NO plays a role in host defense and immunological reactions (Colasanti and Venturini, 1998).

Early evidence of NO production during the innate immune response within invertebrates was demonstrated by Ottaviani *et al.* (1993), in which NO production was increased in molluscan immunocytes after stimulation by *Escherichia coli* LPS. Since then, a number of studies revealing NO production following immune challenge have been reported in other invertebrate organisms, such as the mosquito *Anopheles stephensi* after midgut infection with *Plasmodium* malarial parasites (Luckhart *et al.*, 1998), hemocytes of the crayfish *Procambarus clarkii* following exposure to bacterial LPS (Yeh *et al.*, 2006), hemocytes of the mussel *Mytilus galloprovincinalis* after immune challenge by PAMPs and live bacteria (Costa *et al.*, 2009), and the annelid *Eisenia andrei* after *in vivo* exposure to several immunostimulants (Homa *et al.*, 2013).

The presence of inducible NOS activity has also been identified in a variety of invertebrates, demonstrated in several phyla including mollusks, arthropods, annelids, echinodermates, and nematodes. For example, in an *in vitro* investigation of hemocytes of the spiny lobster *Panulirus argus,* exposure to *E. coli* O55:B5 LPS resulted in an increase in NOS activity and gene expression, which was evaluated by Real Time quantitative polymerase chain reaction (Real Time qPCR). These findings suggest the presence of an inducible form of NOS in these crustacean invertebrates (Rodríguez-Ramos *et al.*, 2010). In addition to NOS enzyme presence, genomic studies have revealed a high degree of sequence similarity in insect NOS genes sequenced so far, with up to 84 % similarity between NOS genes of different insect species (Imamura *et al.*, 2002) and up to 49 % between insect and vertebrate NOS genes (Luckhart and Rosenburg, 1999). These findings provide evidence of a high degree of conservation of the structure and function of the NOS enzymes across the animal kingdom, suggesting that the production of NO through the NOS pathway is a highly conserved mechanism employed during the innate immune response (Rivero, 2006).

The aim of this investigation was to utilize flow cytometry to determine if celomocytes of *E. hortensis* produce NO, a RNI, upon immune stimulation through bacterial challenge *in vitro* to establish whether elicitation of NO production plays a defensive role in earthworms against pathogenic microorganisms. Also, aminoguanidine (hydrochloride), a NOS inhibitor with selectivity for the iNOS isoform, was employed during bacterial exposure to determine if the NOS pathway participates in the synthesis of NO within *E. hortensis* celomocytes. Aminoguanidine functions to inhibit the NOS pathway of intracellular NO synthesis by interacting with conserved glutamine and the guadino group of L-arginine (Griffiths *et al.*, 1993). In invertebrates, aminoguanidine has been previously shown to inhibit inducible NOS activity, such as in the starfish *Asterias forbesi* after NO synthesis was induced through invertebrate interleukin-1-like molecules (Beck *et al.*, 2001). This study provides basic knowledge for more in-depth analysis of defense mechanisms in annelids.

Materials and Methods

Cell culture reagents

Phosphate buffered saline (PBS) (Hyclone) and BD BaculoGold (BG) medium (BD Biosciences) were used for cell culture suspension. BG was supplemented with 10 µg/mL kanamycin (Shelton Scientific), 1X penicillin/streptomycin/amphotericin B (Gibco), 5 µg/mL chloramphenicol (Fluka Biochemika), 10 µg/mL tetracycline (Invitrogen), 1X non-essential amino acids (Gibco), 1X L-glutamine (Gibco), and HEPES buffer (Sigma Aldrich). Final resuspension of earthworm celomocytes was in BG containing 10 % calf serum (BG-S) (Hyclone).

Bacterial culturing and fixation

The soil-dwelling bacterial species used in this study included the Gram positive *Bacillus megaterium* and *Arthrobacter globiformis* and the Gram negative *Pseudomonas stutzeri* and *Azotobacter chroococcum* (Carolina Biological Supply Company and Presque Isle Cultures). Bacterial cultures were generated by inoculating tryptic soy agar (TSA) plates with the stock culture and incubating overnight at 37 °C. From the starter plate, a few colonies were transferred into 10 mL tryptic soy broth (TSB) and incubated overnight on a shaking incubator at 220 rpm, 37 °C. The broth culture was then brought to a 100 mL volume by adding sterile TSB, and placed back on the shaking incubator at 220 rpm, 37 °C for 3 - 5 h to grow bacteria into log phase. Incubation was followed by centrifugation (3273*g*, 5 min, 4 °C), and the cellular pellet was resuspended in 10 % paraformaldehyde in PBS for 1 h. After chemical fixation, the bacteria were washed three times with PBS through centrifugation, followed by a final resuspension in

BG medium. Enumeration was conducted by serial dilution using a hemacytometer and phase-contrast microscopy, which enabled the determination of bacterial concentration. Fixed bacterial samples were stored at 4 °C until needed for use.

Animal husbandry

Eisenia hortensis were purchased from Vermitechnology Unlimited (USDA Permit #52262) and shipped overnight. Short-term colonies of earthworms were kept in habitats containing moistened, autoclaved chipped pine wood bedding, Single Grain Rice Cereal or Oatmeal Banana Cereal (Gerber) for nutrients, and a top layer of shredded, autoclaved paper towels. Colonies were maintained in the dark at a controlled temperature of 20 °C, and the habitats were cleaned twice weekly. Earthworms were euthanized by freezing after extrusion of celomocytes.

Celomocyte extrusion and pre-labeling with DAF-FM DA

The day prior to extrusion of celomocytes from *E. hortensis*, a predetermined number of healthy and active worms were placed by groups of five into a sterile Petri dish containing paper towels saturated with 2.5 µg/mL Fungizone (Fischer Scientific) to minimize the amount of fecal and other contaminants from the earthworm habitat during the extrusion process. The next day, using aseptic technique, each individual earthworm was placed into plastic troughs containing 3 mL of BD FACSFlow sheath fluid (BD Biosciences), which served as an extrusion buffer in which earthworms would become agitated and subsequently release celomocytes from the celomic cavity through the dorsal pores. The celomic suspension (which included both eleocytes and amebocytes) was transferred into 0.5 mL of Accumax™ (Innovative Cell Technologies, Inc.) to obtain single cell suspensions. After a 5 min incubation at room temperature, samples were diluted with 5 mL of PBS, followed by centrifugation (150*g*, 5 min, 4 °C). Celomocytes were then resuspended in 1 mL of BG medium and enumerated with a hemacytometer (Fischer Scientific) through phase-contrast microscopy. Samples containing the highest cell count and lowest proportion of autofluorescent eleocytes were adjusted to $1x10^6$ cells/mL in BG medium in preparation for pre-labeling. In a sterile vial, celomocytes ($1x10^6$/mL) were pre-labeled with the fluorescent indicator 4-amino-5-methylamino-2'7'-difluorofluorescein diacetate (DAF-FM DA) (5 µg/$1x10^6$ celomocytes) (Molecular Probes) and incubated for 90 min on a shaking incubator at 220 rpm, 25 °C. DAF-FM DA reacts with intracellular NO producing a fluorescent benzotriazole derivative. Celomocyte samples were then diluted with BG-S, washed twice, and collected by centrifugation (150*g*, 7 min, 4 °C), followed by final re-suspension in BG-S. As a positive control, the reagent (S)-nitroso-N-acetylpenicillamine (SNAP) (2 µM) was employed in all NO production assays and NOS inhibition assays to provide a source of NO to react with DAF-FM DA.

Nitric oxide (NO) production assays

For each assay conducted, 96-well V-bottom plates were used, with treatments (BG medium, SNAP, or bacteria) performed on celomocytes isolated from individual earthworms, with each treatment conducted in triplicate. Each NO assay employed a range of multiplicities of infection (MOI), which is the ratio between the number of bacteria to celomocytes. Concentrations of bacterial and pre-labeled earthworm cells were adjusted for each desired MOI. The MOIs ranged from 4:1 to 500:1, with three different MOIs used in each assay in order to detect a dose response of NO production in *E. hortensis* celomocytes. 100 µL of the specified celomocyte sample ($1x10^5$ celomocytes) and 100 µL of the respective treatment solution (bacteria at desired MOI, SNAP, or BG medium) was added and thoroughly mixed within each well. Additional negative controls included wells with unlabeled celomocytes only, bacteria only, and a combination of the two, in order to measure the autofluorescent background. The plates were incubated for 16-18 h in 5 % CO_2 at 25 °C. Following incubation, assay plates were centrifuged (150*g*, 7 min, 4 °C) and celomocytes were resuspended in 200 µL of ice-cold PBS. The samples were then transferred into flow cytometry tubes containing 50 µL FACSFlow buffer, placed on ice, kept in the dark, and run immediately on the flow cytometer.

Nitric oxide synthase (NOS) inhibition assays

Pre-labeled celomocytes ($1x10^5$ in 100 µL) were added to wells of a 96-well V-bottom plate. Treatment was performed on pre-labeled celomocytes isolated from individual earthworms and conducted in triplicate. 50 µL of the NOS inhibitor aminoguanidine hydrochloride (AG) (Cayman Chemical Company) at a final concentration of 1000 µM or 200 µM was added to specified celomocyte samples in each respective treatment wells, followed by a 1 h incubation at 25 °C, 5 % CO_2. After pre-incubation with AG, 50 µL of *B. megaterium* at an MOI of 200:1 was added to each respective treatment well. The same negative and positive controls as described above for NO production assays were also employed in each NOS inhibition assay. An uninhibited NO production control was also performed in triplicate, which included wells containing pre-labeled celomocytes with 50 µL *B. megaterium* (200:1 MOI) and 50 µL BG medium. The plates were incubated for 16-18 h at 25 °C, 5 % CO_2. Following incubation, plates were centrifuged (150*g*, 7 min, 4 °C) and celomocytes were resuspended in 200 µL of ice-cold PBS and prepared for flow cytometry as described for NO production assays.

In order to ensure that AG did not exhibit cytotoxic effects on celomocytes during the incubation period, the fluorescent viability dye 7-aminoactinomycin D (7-AAD) (1.25 µL per $1x10^5$ celomocytes) was added just prior to collection of celomocytes on the flow cytometer. Fluorescence in FL-3 depicted uptake of 7-AAD by nonviable, membrane-compromised celomocytes. The detergent saponin (0.02 %) was included as a positive control in order to set quadrant statistical markers at the appropriate threshold to distinguish live from dead cells.

Data acquisition - flow cytometry

A FACSCalibur flow cytometer and Cell Quest Pro software (BD Biosciences) were used for all assays. Voltages for forward scatter (FSC) correlating to cellular size, side scatter (SSC) correlating to granularity, and FL-1, which detects the green fluorescence of the benzotriazole derivative formed by the reaction of DAF-FM DA with intracellular NO, were set by previewing the negative control samples on set-up mode, and adjusting the threshold value in order to eliminate, as much as possible, bacteria from data acquisition. In order to concentrate solely on the relevant celomocyte subpopulation, a region (R1) was placed around the area corresponding to the amebocyte population on a dot plot of FSC versus SSC, based upon previous understanding of the size and granularity of relevant amebocyte cells. This also enabled the exclusion of unwanted events during data collection, such as bacteria, cellular debris, and highly autofluorescent eleocytes (Fig. 1A). A maximum of 10,000 events per sample was collected. A histogram of the baseline control gated on R1 was created, showing relative fluorescence intensity (RFI) detected in FL-1 in log scale (abscissa) versus the cell count (ordinate) (Fig. 1B). The RFI values correlate to the concentration of NO within each cell. On the histogram, a marker (M1) was set to facilitate acquisition of the geometric mean of RFI of the entire amebocyte population. An example is shown in Figure 1B, in which the geometric mean of the RFI of the representative sample was 32.90. Figure 1C depicts a histogram of the positive control, SNAP, of the representative sample, with a geometric mean of RFI of 74.06, a clear increase in RFI compared to the baseline control sample. For NOS inhibition assays, data of cell viability were also acquired by flow cytometry through the FL-3 detector, which measured fluorescence of the viability dye 7-AAD. A region (R1) was set around the relevant celomocyte population, as described in NO production assays (Fig. 2A). A dot plot of FSC (abscissa) versus 7-AAD (FL-3, ordinate), which was gated on R1, provided the means to distinguish live from dead cells within the respective population. Live cells do not take up the 7-AAD dye, and are therefore FL-3 negative (lower right quadrant), while dead cells do take up 7-AAD, and are therefore FL-3 positive (upper right quadrant). Figure 2B shows 88.30 % viable celomocytes. Quadrant placement was guided by the shift in RFI upon treatment with the membrane-destabilizing detergent saponin, as shown in Figure 2C where the majority of cells reside in the upper right quadrant (nonviable) and only 0.95 % are in the lower right quadrant (viable).

Statistical analysis

In Microsoft Excel 2010, the t-test: paired two-sample for means was used to determine statistical significance of the data obtained. In all NO production assays, the geometric mean of RFI values for each triplicate set of treatment wells (bacteria or SNAP) was compared to the geometric mean of RFI values for each triplicate set of baseline control wells of the same earthworm amebocyte population. For NOS inhibition assays, the same statistical analyses were performed, with the addition of the comparison between the geometric mean of RFI values of each triplicate set of inhibitor treatment wells (AG plus *B. megaterium*) and the geometric mean of RFI values of each triplicate set of bacteria treatment wells (*B. megaterium* only) of the same earthworm amebocyte population. The average RFI value and standard deviation of each triplicate set of samples pertaining to a particular control or treatment was determined and recorded in tabular format. Statistical significance was granted to resulting p-values within particular treatments that were less than or equal to 0.05, indicating a 95 % confidence interval.

Results

Measurement of levels of autofluorescence in bacterial samples

Figure 3 demonstrates that the four bacteria used in this study (*B. megaterium, A. globiformis, P. stutzeri,* and *A. chroococcum*) were not autofluorescent, nor did they contribute to an increase in RFI in FL-1 when combined with unlabeled amebocytes and incubated together for 16 - 18 h. It was important during data acquisition to exclude as much as possible bacteria, cellular debris, autofluorescent eleocytes, and cellular aggregates, and to ensure that the data that was acquired was restricted to the amebocyte population for final analysis of NO production. The high forward scatter (FSC) threshold that was set on the flow cytometer during cell acquisition facilitated the exclusion of the majority of the bacteria from the final data collection set. In addition, it was important to establish that the amebocytes and bacteria used in this study did not contribute significant levels of autofluorescence to the fluorescence generated by the amebocytes during the period of treatment. Note that when the four bacterial samples were run on their own, there was minimal overlap of cellular events in R1, the region upon which FL-1 histograms were subsequently gated (see Materials and Methods for description of data collection).There was little, if any, effect on the RFI of the amebocytes when incubated with bacteria (Fig. 3, left versus right panels). Therefore, these results show that the background fluorescence of the unlabeled amebocytes, free bacteria, or the combination of the two was negligible. In addition, because the bacteria were pretreated with paraformaldehyde, their metabolic ability to produce NO was incapacitated.

Earthworm amebocytes produce NO in response to bacterial challenge

In order to determine if earthworm amebocytes possess the ability to synthesize NO upon exposure to bacteria, NO assays were conducted by incubating amebocytes extruded from individual earthworms with four different bacterial species of soil-dwelling bacteria which were pretreated with paraformaldehyde. A minimum of three separate assays in which *E. hortensis* amebocytes were incubated overnight (16 h) with each bacterium at a range of MOIs were performed to demonstrate inter-assay reliability and reproducibility. Pre-labeling amebocytes with the fluorescent indicator DAF-FM DA facilitated the measurement of the RFI value by the FL-1 detector in each amebocyte sample through

A.

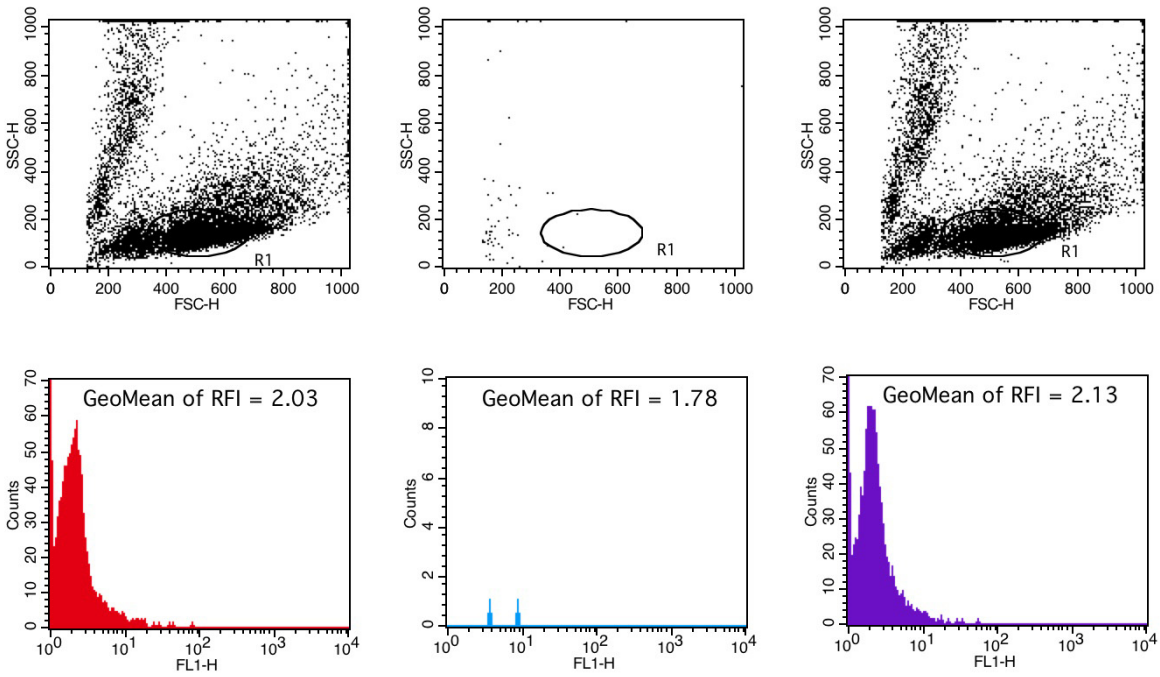

Unlabeled Amebocytes Only

B. megaterium Only

Amebocytes plus *B. megaterium*

B.

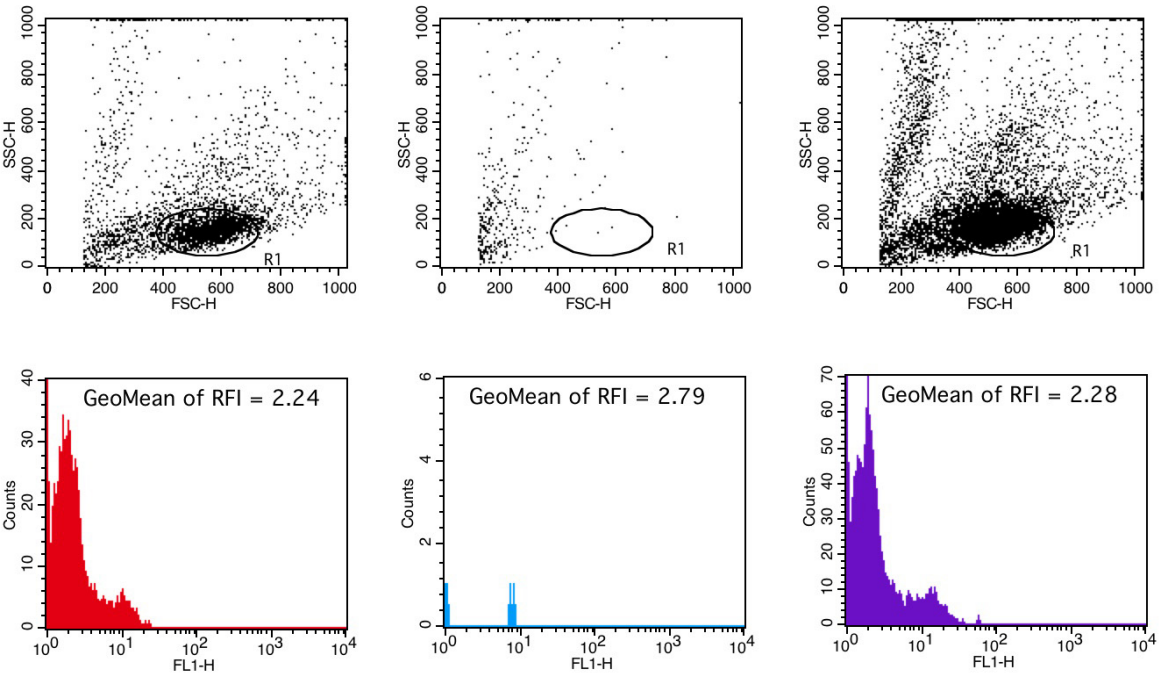

Unlabeled Amebocytes Only

A. globiformis Only

Amebocytes plus *A. globiformis*

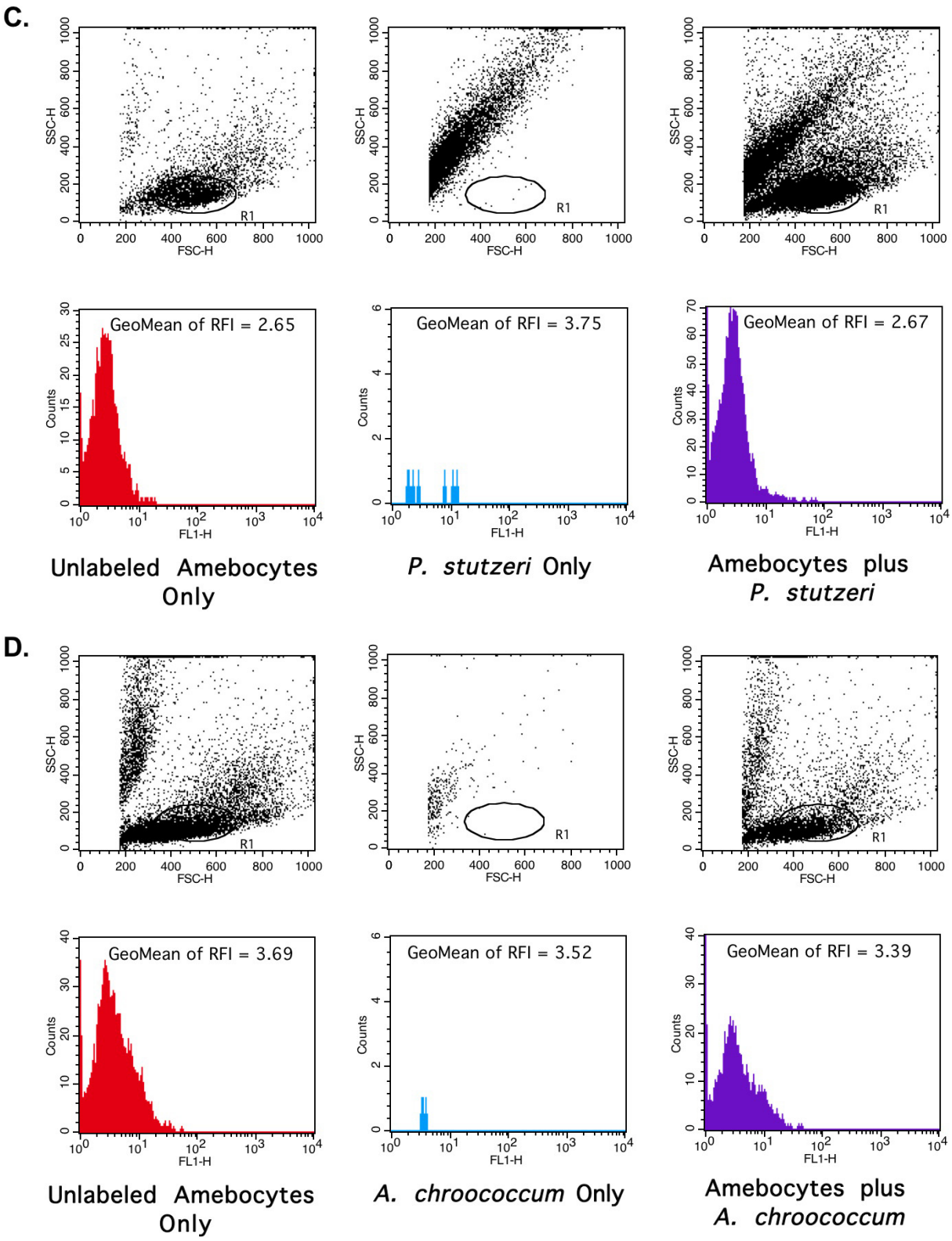

Fig. 3 Autofluorescent flow cytometry controls and placement of region (R1). Data shown in A-D are representative of all bacteria used in this study. A and B represent Gram positive *B. megaterium* and *A. globiformis*, respectively. C and D represent Gram negative *P. stutzeri* and *A. chroococcum,* respectively. In each case there are six panels that correspond to FSC (abscissa) versus SSC (ordinate) (top row), and R1-gated FL-1 (abscissa) versus cell number (ordinate) (bottom row). The top row shows unlabeled (no DAF-FM DA) earthworm celomocytes, bacteria, and the combination of the two in the left, middle, and right panels, respectively. Also shown is the placement of R1. The bottom row presents the corresponding R1-gated FL-1 histograms for the unlabeled earthworm amebocytes, bacteria, and the combination of the two in the left, middle, and right panels, respectively. Also shown is the geometric mean of the RFI (FL-1).

A.

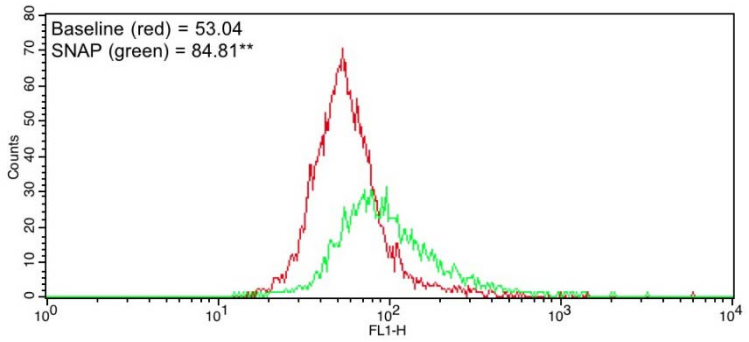
Baseline (red) = 53.04
SNAP (green) = 84.81**
Counts
FL1-H

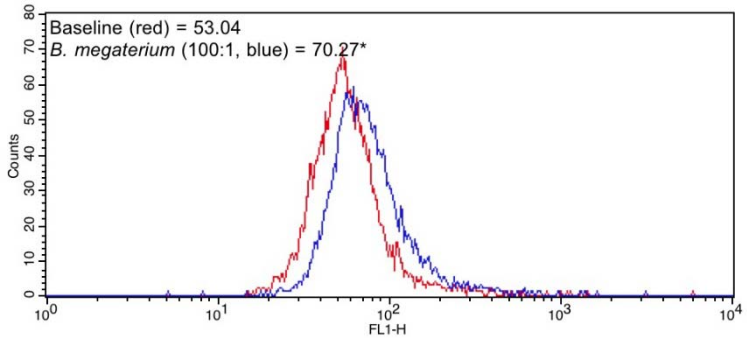
Baseline (red) = 53.04
B. megaterium (100:1, blue) = 70.27*
Counts
FL1-H

B.

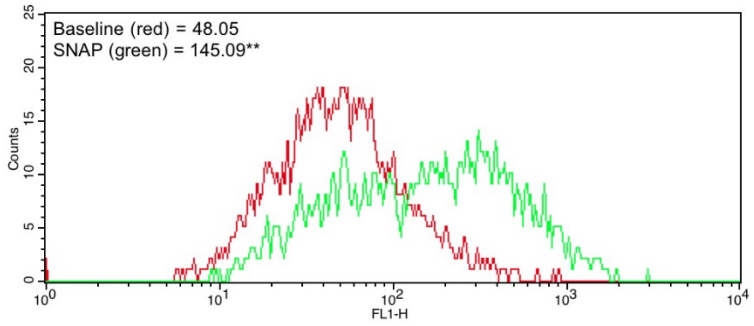
Baseline (red) = 48.05
SNAP (green) = 145.09**
Counts
FL1-H

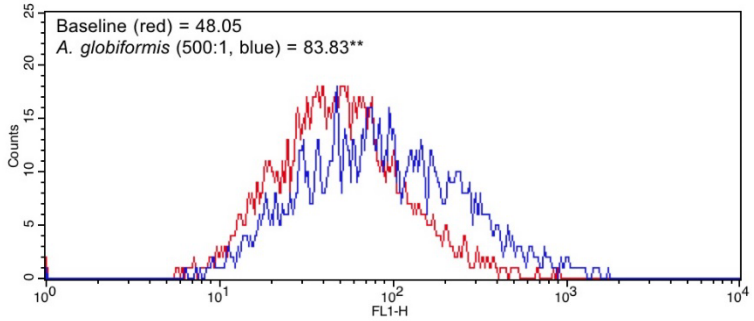
Baseline (red) = 48.05
A. globiformis (500:1, blue) = 83.83**
Counts
FL1-H

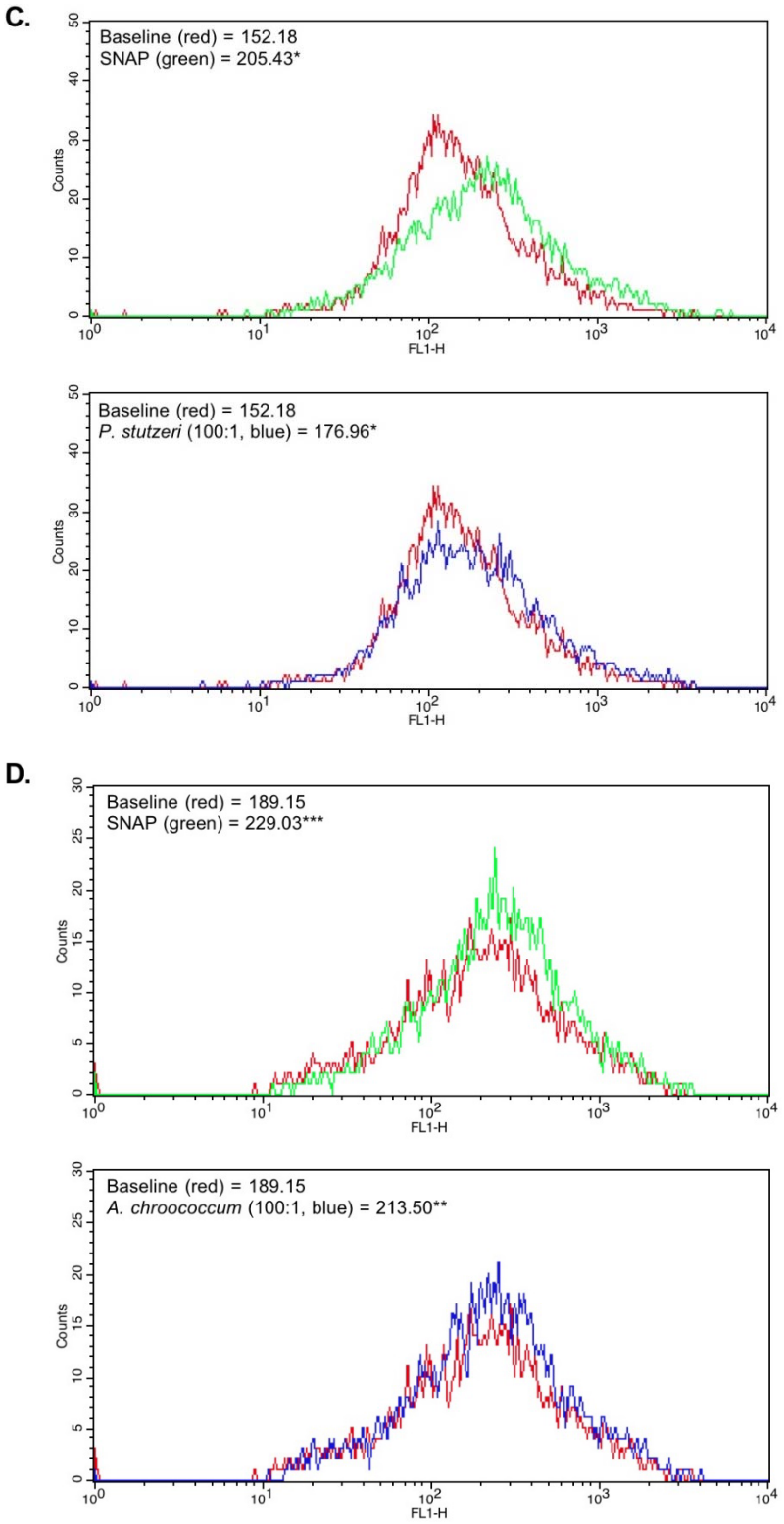

Fig. 4 Histogram overlays of NO production in amebocyte populations stimulated with bacteria. Data shown in A-D are representative of R1-gated, FL-1 histogram overlays of baseline (red) versus positive control (SNAP, green) (top panel), and baseline (red) versus bacteria-treated amebocytes (blue) (bottom panel). *B. megaterium* used at an MOI of 100:1 is shown in A. *A. globiformis* used at an MOI of 500:1 is shown in B. *P. stutzeri* used at an MOI of 100:1 is shown in C. *A. chroococcum* used at an MOI of 100:1 is shown in D. The geometric mean of the RFI (FL-1) is included. Asterisks indicate statistical significance (* = $p \leq 0.05$; ** = $p \leq 0.005$; and *** = $p \leq 0.0005$) as determined by student's t test: paired two samples for means.

Table 1 Average geometric mean of RFI values (± standard deviation) of NO assays measured in FL-1 after overnight (13 - 16 h) incubation with *B. megaterium*

				Multiplicity of Infection (MOI)				
		Baseline	**SNAP**	**Bm 100:1**	**Bm 50:1**	**Bm 25:1**	**Bm 10:1**	**Bm 1:1**
Assay A	**EW 1**	57.77 (±4.28)	80.19 (±6.09)**	68.59 (±1.67)*	64.45 (±1.35)	62.56 (±0.40)	NT	NT
	EW 2	45.58 (±1.03)	73.44 (±2.08)***	56.15 (±0.36)**	51.26 (±0.78)*	49.79 (±0.76)**	NT	NT
	EW 3	87.53 (±5.57)	159.59 (±11.79)**	119.14 (±0.93)**	101.09 (±6.34)**	93.46 (±3.35)*	NT	NT
Assay B	**EW 4**	52.07 (±0.53)	85.24 (±2.33)**	71.80 (±3.70)*	62.65 (±1.79)*	57.74 (±0.77)**	NT	NT
	EW 5	116.02 (±1.31)	108.81 (±0.76)	131.47 (±1.19)**	124.68 (±5.25)	120.74 (±3.20)*	NT	NT
	EW 6	50.59 (±2.84)	81.27 (±3.25)**	66.36 (±2.36)**	60.23 (±1.36)*	60.53 (±2.10)*	NT	NT
Assay C	**EW 7**	76.57 (±0.39)	114.51 (±5.01)**	89.78 (±1.64)**	NT	NT	81.21 (±1.56)*	77.51 (±1.90)
	EW 8	102.03 (±5.90)	141.86 (±4.42)**	132.13 (±1.90)**	NT	NT	104.41 (±3.20)	105.91 (±3.07)
	EW 9	32.02 (±1.05)	55.04 (±1.92)**	40.66 (±0.41)**	NT	NT	33.13 (±0.61)*	31.31 (±0.12)
Assay D	**EW 10**	33.02 (±2.44)	35.26 (±2.97)	38.29 (±0.31)*	NT	NT	33.5 (±1.51)	33.11 (±0.77)
	EW 11	112.80 (±1.85)	126.54 (±2.77)*	124.15 (±3.24)*	NT	NT	119.67 (±1.19)*	116.05 (±2.36)
	EW 12	63.86 (±1.61)	70.20 (±5.83)	73.72 (±2.00)*	NT	NT	68.60 (±0.63)*	64.86 (±0.75)

The geometric mean of RFI corresponds to the concentration of NO present within each earthworm (EW) sample. The RFI values of each baseline negative control sample were compared to the RFI value of the positive control sample, SNAP, and the RFI values in amebocyte samples exposed to *Bacillus megaterium* (Bm) at different MOIs in two- or ten-fold serial dilutions. Each sample was gated on R1 to include amebocytes only, excluding other cell populations. The results of four separate NO assays are included. Statistically significant NO levels above the baseline control are indicated as: * = $p \leq 0.05$; ** = $p \leq 0.005$; and *** = $p \leq 0.0005$, as determined by student's t test: paired two samples for means. (NT = not tested).

flow cytometric analysis (refer to Figure 1 for an explanation of data analysis). The average RFI value, which reflects the concentration of intracellular NO, was calculated from each triplicate set of pre-labeled amebocytes following treatment with media (baseline control), SNAP (positive control), or bacteria. Statistical analyses were performed to determine if the positive differences in the mean RFI value, and therefore NO concentration, between the pre-labeled baseline control amebocytes and the pre-labeled stimulated amebocytes (SNAP or bacteria) were statistically significant as determined by the student's t-test: paired two sample for means. Significant increases in RFI values above the baseline controls, which represents an increase in the production of NO, was observed following amebocyte stimulation with all bacterial species used at the MOIs tested.

Figures 4A and 4B illustrate representative histogram overlays of pre-labeled amebocyte samples from the same individual earthworm following incubation with Gram positive bacteria *B. megaterium* (A) and *A. globiformis* (B). The top histogram overlays of 4A and 4B demonstrate NO production in amebocytes incubated with the positive control SNAP (green) above the baseline control (red). The bottom histogram overlays also show

Table 2 Average geometric mean of RFI values (± standard deviation) of NO assays measured in FL-1 after overnight (13 - 16 h) incubation with *A. globiformis*

				Multiplicity of Infection (MOI)			
		Baseline	**SNAP**	**Ag 500:1**	**Ag 100:1**	**Ag 20:1**	**Ag 4:1**
Assay A	**EW 1**	107.04 (±0.27)	139.39 (±1.67)*	NT	113.07 (±0.40)*	108.84 (±4.47)	105.79 (±0.47)
	EW 2	74.87 (±2.43)	126.79 (±3.08)**	NT	77.45 (±5.70)	73.40 (±2.03)	70.92 (±3.81)
	EW 3	82.04 (±2.53)	110.87 (±2.49)***	NT	76.43 (±1.34)	79.66 (±1.73)	N/A
Assay B	**EW 4**	75.16 (±1.18)	107.8 (±3.11)**	87.86 (±1.23)**	70.22 (±2.97)*	68.47 (±0.78)	NT
	EW 5	205.37 (±3.72)	215.08 (±7.13)*	243.25 (±12.11)*	204.36 (±9.59)	190.22 (±3.86)	NT
	EW 6	48.34 (±0.25)	133.40 (±10.13)**	82.69 (±1.43)***	56.01 (±1.00)**	48.78 (±0.16)	NT
Assay C	**EW 7**	258.76 (±5.58)	382.94 (±12.51)**	286.05 (±2.64)*	264.15 (±29.75)	235.78 (±17.63)	NT
	EW 8	108.79 (±6.78)	159.2 (±13.12)*	130.62 (±6.44)*	120.68 (±7.84)	113.79 (±0.83)	NT
	EW 9	564.85 (±15.34)	683.53 (±36.81)*	687.35 (±24.63)*	648.04 (±12.65)**	584.40 (±7.03)*	NT

The geometric mean of RFI corresponds to the concentration of NO present within each earthworm (EW) sample. The RFI values of each baseline negative control sample were compared to the RFI value of the positive control sample, SNAP, and the RFI values in amebocyte samples exposed to *Arthrobacter globiformis* (Ag) at different MOIs in five- or ten-fold serial dilutions. Each sample was gated on R1 to include amebocytes only, excluding other cell populations. The results of three separate NO assays are included. Statistically significant NO levels above the baseline control are indicated as: * = $p \leq 0.05$; ** = $p \leq 0.005$; and *** = $p \leq 0.0005$, as determined by student's t test: paired two samples for means. (NT = not tested).

increases in NO production after amebocytes were incubated with *B. megaterium* at an MOI of 100:1 (A, blue) or *A. globiformis* at an MOI of 500:1 (B, blue) compared to baseline controls (red). The mean RFI values of all amebocyte samples from NO production assays following Gram positive bacterial stimulation at all MOIs tested are summarized in Table 1 (*B. megaterium*) and Table 2 (*A. globiformis*).

Based on the same format described for Figures 4A and 4B, 4C and 4D demonstrate representative histogram overlays of pre-labeled amebocyte samples following incubation with SNAP (top histograms) or Gram negative bacteria (bottom histograms) *P. stutzeri* (C) or *A. chroococcum* (D). Significant increases in RFI values in amebocytes stimulated with both Gram negative bacteria, *P. stutzeri* used at an MOI of 100:1 (C, blue) and *A. chroococcum* used at an MOI of 100:1 (D, blue), above baseline controls (red) were observed. The mean RFI values of all amebocyte samples from NO production assays following Gram negative bacterial stimulation at all MOIs tested are summarized in Table 3 (*P. stutzeri*) and Table 4 (*A. chroococcum*).

The percentage of statistically significant responses of NO production upon amebocyte stimulation with bacteria was generally dependent on the MOI employed. Our results of NO production show a dose-response relationship in which the percentage of statistically significant increases in RFI values above baseline controls decreased as the bacterial MOI decreased. In the cases of Gram positive bacterial exposure, statistically significant increases in RFI values were observed in 100 % (n = 12) of earthworms treated with *B. megaterium* at an

Table 3 Average geometric mean of RFI values (± standard deviation) of NO assays measured in FL-1 after overnight (13 - 16 h) incubation with *P. stutzeri*

				Multiplicity of Infection (MOI)		
		Baseline	**SNAP**	**Ps 100:1**	**Ps 20:1**	**Ps 4:1**
Assay A	**EW 1**	78.61 (±1.41)	114.78 (±7.69)*	82.69 (±2.95)*	77.13 (±0.46)	78.81 (±1.83)
	EW 2	42.60 (±0.45)	58.33 (±1.26)**	52.59 (±1.36)**	44.89 (±0.99)*	44.67 (±0.90)*
	EW 3	62.55 (±1.19)	77.13 (±1.42)**	70.57 (±1.92)**	62.78 (±1.54)	63.08 (±2.78)
Assay B	**EW 4**	33.78 (±0.68)	34.92 (±0.84)	37.62 (±0.85)*	34.25 (±0.56)	32.95 (±1.12)
	EW 5	154.27 (±2.45)	196.42 (±12.40)*	174.21 (±2.81)*	152.74 (±3.89)	154.96 (±7.28)
	EW 6	199.31 (±7.47)	245.68 (±1.91)**	208.33 (±3.90)*	196.48 (±5.95)	195.43 (±5.46)
Assay C	**EW 7**	503.83 (±0.83)	409.38 (±13.00)	444.02 (±12.54)	435.39 (±3.56)	444.05 (±17.42)
	EW 8	562.46 (±20.76)	430.01 (±7.40)	563.9 (±17.47)	564.08 (±18.89)	548.0 (±13.97)
	EW 9	308.02 (±10.50)	298.34 (±7.16)	315.61 (±7.49)	311.83 (±1.58)	305.97 (±4.84)

The geometric mean of RFI corresponds to the concentration of NO present within each earthworm (EW) sample. The RFI values of each baseline negative control sample were compared to the RFI value of the positive control sample, SNAP, and the RFI values in amebocyte samples exposed to *Pseudomonas stutzeri* (Ps) at different multiplicities of infection (MOI) in five-fold serial dilutions. Each sample was gated on R1 to include amebocytes only, excluding other cell populations. The results of three separate NO assays are included. Statistically significant NO levels above the baseline control are indicated as: * = $p \leq 0.05$; ** = $p \leq 0.005$; and *** = $p \leq 0.0005$, as determined by student's t test: paired two samples for means. (NT = not tested).

MOI of 100:1 compared to baseline control. In contrast, only 67 % (n = 6), 83 % (n = 6), and 67 % (n = 6) of earthworms exhibited significant increases in NO at lower MOIs of 50:1, 25:1, and 10:1, respectively. A similar pattern was observed when amebocytes were stimulated with *A. globiformis,* where 100 % (n = 6), 44 % (n = 9), and 11 % (n = 9) of all earthworms exhibited significant increases in RFI values compared to baseline control at MOIs of 500:1, 100:1, and 20:1, respectively. Lower incidences of significant responses were observed in cases employing Gram negative bacterial challenge, where only 67 % (n = 9) and 11 % (n = 9) of all earthworms stimulated with *P. stutzeri* at MOIs of 100:1 and 20:1, respectively, exhibited statistically significant increases in RFI values above baseline control. Likewise, of all earthworms stimulated with *A. chroococcum*, only 50 % (n = 8), 27 % (n = 11), and 18 % (n = 11) exhibited statistically significant increases in RFI values compared to baseline controls at MOIs of 500:1, 100:1, and 20:1, respectively.

These results demonstrate that pre-labeled amebocytes stimulated with both Gram positive and Gram negative bacteria exhibited statistically significant increases in NO production compared to baseline controls. A greater percentage of statistically significant responses of NO production were observed in amebocytes after Gram positive stimulation than after Gram negative stimulation, and *B. megaterium* stimulated 100 % significant responses at an MOI of 100:1. Based on the consistent response rate obtained with *B. megaterium*, this bacterium was selected for the next experiment utilizing the NOS inhibitor aminoguanidine.

Table 4 Average geometric mean of RFI values (± standard deviation) of NO assays measured in FL-1 after overnight (13 - 16 h) incubation with *A. chroococcum*

				Multiplicity of Infection (MOI)			
		Baseline	**SNAP**	**Ac 500:1**	**Ac 100:1**	**Ac 20:1**	**Ac 4:1**
Assay A	**EW 1**	191.40 (±1.96)	227.21 (±1.78)***	NT	209.62 (±3.51)**	192.02 (±5.60)	194.92 (±2.09)
	EW 2	256.26 (±2.12)	324.11 (±7.07)**	NT	249.30 (±30.82)	251.82 (±3.93)	248.36 (±6.68)
	EW 3	164.92 (±0.88)	206.22 (±7.94)**	NT	176.00 (±4.62)*	169.03 (±1.51)**	166.25 (±1.04)*
Assay B	**EW 4**	199.85 (±5.93)	254.13 (±6.65)*	197.00 (±4.75)	187.75 (±1.32)	195.01 (±1.10)	NT
	EW 5	524.09 (±12.55)	700.71 (±54.47)*	482.74 (±15.09)	482.22 (±21.37)	487.23 (±12.75)	NT
	EW 6	57.03 (±1.80)	78.21 (±3.90)*	54.81 (±0.64)	54.62 (±0.25)	55.71 (±1.42)	NT
Assay C	**EW 7**	37.29 (±1.04)	47.23 (±1.31)***	42.81 (±2.71)*	37.65 (±1.82)	40.17 (±0.55)***	NT
	EW 8	12.90 (±0.59)	14.57 (±0.69)*	13.53 (±0.28)	12.72 (±0.23)	13.09 (±0.10)	NT
Assay D	**EW 9**	416.1 (±0.43)	362.07 (±2.23)	547.93 (±10.79)**	435.67 (±13.25)	400.68 (±10.35)	NT
	EW 10	422.85 (±9.41)	373.45 (±3.06)	571.72 (±11.12)**	444.32 (±8.30)	379.75 (±46.81)	NT
	EW 11	264.71 (±6.02)	264.42 (±10.13)	337.4 (±33.37)*	290.90 (±3.95)**	265.25 (±4.28)	NT

The geometric mean of RFI corresponds to the concentration of NO present within each earthworm (EW) sample. The RFI values of each baseline negative control sample were compared to the RFI value of the positive control sample, SNAP, and the RFI values in amebocyte samples exposed to *Azotobacter chroococcum* (Ac) at different multiplicities of infection (MOI) in five- or ten-fold serial dilutions. Each sample was gated on R1 to include amebocytes only, excluding other cell populations. The results of four separate NO assays are included. Statistically significant NO levels above the baseline control are indicated as: * = $p \leq 0.05$; ** = $p \leq 0.005$; and *** = $p \leq 0.0005$, as determined by student's t test: paired two sample for means. (NT = not tested).

Aminoguanidine hydrochloride inhibits NO production in a dose-dependent manner

The NOS inhibitor aminoguanidine (AG) was employed in NO inhibition assays to determine if *E. hortensis* utilize a similar pathway of NO synthesis as other vertebrate and invertebrate organisms during the innate immune response. Two assays were conducted in which a total of twelve individual earthworms were included to determine if AG inhibited the increased production of NO after bacterial stimulation. Amebocytes pre-labeled with DAF-FM DA were pre-incubated with AG at concentrations of 1,000 µM or 250 µM followed by a 16 h incubation with *B. megaterium* at an MOI of 200:1. NO production by amebocyte samples treated with media (baseline control), SNAP, bacteria only, or a combination of bacteria plus AG was measured through flow cytometric analysis, as previously described. Figures 5A and 5B illustrate histogram overlays of amebocytes of an individual earthworm depicting a statistically significant increase in mean RFI value measured in FL-1 above baseline control (red, Fig. 5A) upon stimulation with *B. megaterium* at an MOI of 200:1 (blue, Figs 5A and 5B), and a statistically significant decrease in mean RFI value upon a pre-incubation of AG at a concentration of 1,000 µM (orange, Fig. 5B). The first statistical analysis was performed to determine if the differences between the mean RFI values of the amebocyte samples treated with either SNAP or *B. megaterium* only compared to baseline controls were statistically significant (shown as blue asterisks),

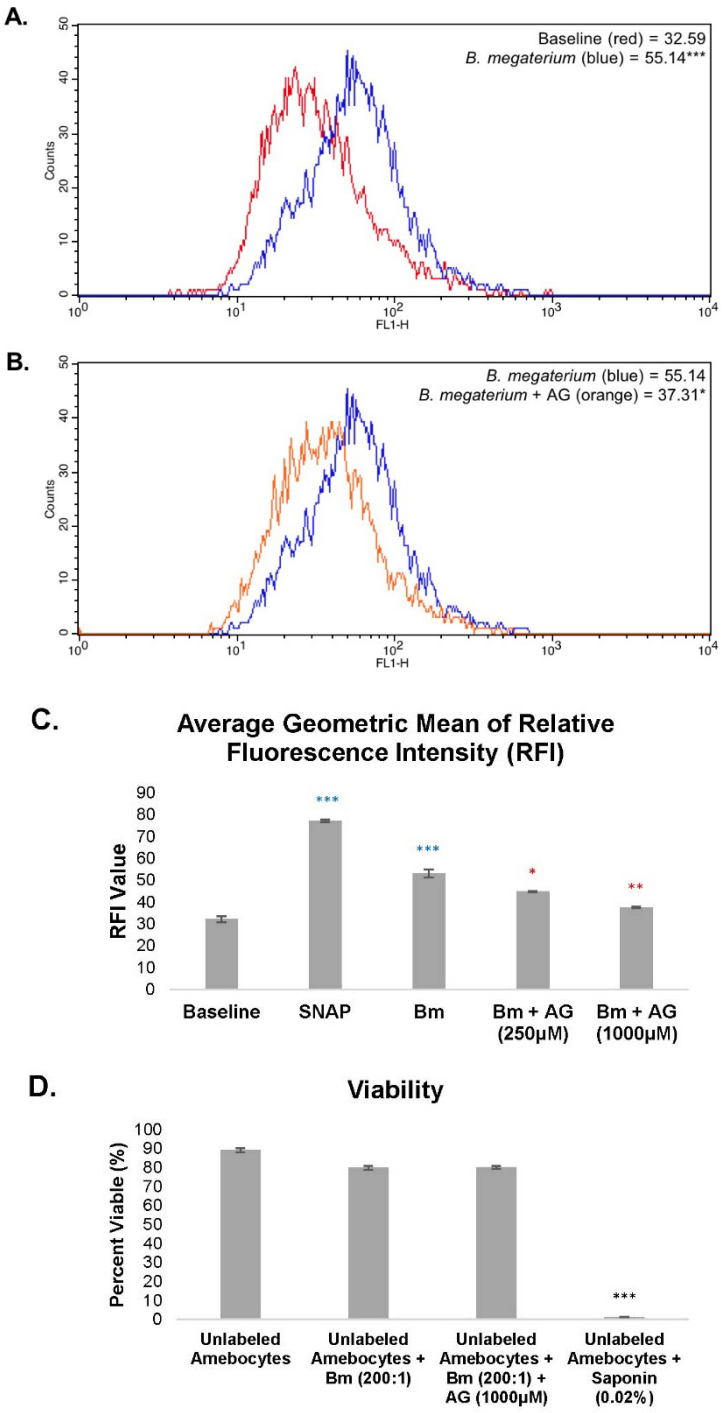

Fig. 5 Treatment of amebocytes with the NOS inhibitor aminoguanidine hydrochloride (AG) and viability controls. Panel A shows R1-gated histogram overlays of RFI (FL-1, abscissa) versus cell number (ordinate) of the baseline control sample (red) compared to amebocytes stimulated with *B. megaterium* at an MOI of 200:1 (blue). Panel B shows histogram overlays (as described above) of RFI of the *B. megaterium*-stimulated amebocyte sample (blue) compared to the RFI of the *B. megaterium*-stimulated amebocyte sample containing the NOS inhibitor AG (1,000 µM, orange). Panel C shows RFI of the baseline, SNAP control, *B. megaterium* (MOI 200:1) in the absence or presence of AG at two different concentrations (250 µM or 1,000 µM). Blue asterisks denote significant increases in RFI of SNAP-treated or bacteria-treated samples compared to baseline controls. Red asterisks denote significant decreases in RFI of samples treated with bacteria plus aminoguanidine compared to bacteria only. Panel D shows the results of a viability test to measure toxicity of AG at 1,000 µM using the same population exhibited in panels A-C. Amebocytes were incubated with AG for the same time course as the inhibitor assay and subsequently labeled with 7-AAD before being run on the flow cytometer. Percent viability (as described in Fig. 2) is shown for R1-gated amebocytes alone, with *B. megaterium* (MOI 200:1), with *B. megaterium* plus AG, or saponin. Asterisks indicate statistical significance (* = $p \leq 0.05$; ** = $p \leq 0.005$; and *** = $p \leq 0.0005$) as determined by student's t test: paired two samples for means.

indicating a significant increase in NO production. Only in the case of those bacteria-stimulated amebocyte samples which exhibited significant increases in NO production above the baseline controls, was a second statistical analysis performed. The second t-test determined decreases in NO production in those samples treated with AG (1,000 µM or 250 µM) compared to samples not treated with AG. Based on these restrictions, 9 of the 12 amebocyte samples were subjected to both statistical tests. The results demonstrate that after incubation with AG at concentrations of 1,000 µM or 250 µM, 89 % and 44 %, respectively, of amebocyte samples (shown as red asterisks) exhibited significant decreases in NO production compared to samples stimulated with *B. megaterium* and not receiving AG (red asterisks). The decrease in NO production in earthworm amebocytes was dependent on the concentration of AG. As the concentration of AG increased, the RFI values in immune-stimulated amebocytes decreased, as shown in Figure 5C. Table 5 summarizes the results obtained from the 16 amebocyte samples used in this study.

The cytotoxicity of AG was also monitored through the use of the viability dye 7-aminoactinomycin D (7-AAD). A representative sample is shown in Figure 5D. Due to the high degree of spectral overlap of DAF-FM DA in the FL-3 detector of the flow cytometer (which was the detector used for measuring uptake of the viability dye 7-AAD), the measurement of bot fluorochromes simultaneously could not be conducted. Therefore, some of the amebocytes from the same population undergoing exposure to aminoguanidine were not labeled with DAF-FM DA in the viability tests; instead, they were stained with only 7-AAD at the end of the incubation period. Figure 5D shows that the percent of cells exhibiting viability following treatment with media (baseline control), *B. megaterium* only, or a combination of *B. megaterium* plus AG (1,000 µM) is very similar between the three groups and exhibits no significant difference. Table 6 summarizes the results obtained after flow cytometric analysis (as described in Fig. 2) and depicts the percentage of viable amebocytes after treatment with medium only (baseline control), *B. megaterium* (MOI of 200:1) only, a combination of *B. megaterium* plus the inhibitor AG, or saponin. Overall, our results indicate that the NOS inhibitor AG had minimal effect, if any, on the viability of the amebocytes in culture, as demonstrated by the minimal difference observed in percentage of viable cells between the control amebocyte samples and the AG-treated amebocyte samples.

Discussion

This study demonstrates induced production of NO in earthworm celomocytes following exposure to soil-dwelling bacteria. These results suggest that inducible NO plays a role in the immune response of annelids. Similar increases in NO synthesis following immune stimulation have previously been observed in other invertebrate organisms, such as the silkworm *Bombyx mori* (Choi *et al.*, 1995), the mosquito *Anopheles stephensi* (Akman-Anderson, Olivier, and Luckhart, 2007), and the freshwater snail *Viviparus ater* (Conte and Ottaviani, 1995). Due to the wide distribution of NO in other phyla of the animal kingdom, NO is considered to be an important ancestral molecule of the innate immune system (Colasanti and Venturini, 1998). Furthermore, the high degree of conservation of NOS enzymes, both structurally and functionally, across both invertebrate and vertebrate organisms suggests that all could have originated from a single NOS type (Rivero, 2006). This study which investigated NO production and NOS inhibition provides important information on the mechanisms of innate immune responses of invertebrates and on the link between the invertebrate and vertebrate immune systems.

Significant increases in NO production were observed following exposure of *E. hortensis* celomocytes to each species of bacteria used. In our study, we observed greater responses of NO production in amebocytes stimulated by the Gram positive bacteria *B. megaterium* and *A. globiformis* compared to the Gram negative bacteria *P. stutzeri* and *A. chroococcum*. Our results also show that there was a strong correlation between the NO produced and the MOI employed, demonstrating a dose-response relationship. Amebocytes exhibited the highest degree of sensitivity to *B. megaterium,* where an MOI of only 10:1 induced a significant response rate in 67 % of earthworms tested. This rate increased to 100 % at an MOI of 100:1. In contrast, at an MOI of 100:1, *A. globiformis, P. stutzeri,* and *A. chroococcum* induced a significant response in only 44 %, 67 %, and 27 % of sample tested, respectively. Our results parallel those observed in an *in vivo* study in which increased NO production was observed in *E. andrei* celomocytes following dermal exposure to the immunostimulants phorbol-12-myristate-13-acetate (PMA) or concanavalin A (ConA) (Homa *et al.*, 2013). However, we believe that the present study is the first describing the use of a flow cytometric approach to quantify NO production in earthworm celomocytes following *in vitro* bacterial challenge.

We have also shown that incubation of *B. megaterium*-stimulated earthworm celomocytes with the NOS inhibitor aminoguanidine hydrochloride (AG) resulted in significant decreases of NO production compared to controls. We believe that this effect was due to the inhibition of the NOS enzyme, which is responsible for the production of NO. A correlation in the concentration of AG and the production of NO was also observed in the NOS inhibition assays, in which a greater decrease in NO production occurred in amebocytes exposed to the high concentration of AG used (1,000 µM) compared to the low concentration (250 µM). To control for possible cytotoxic effects of AG, a viability test was included within each NOS inhibition assay. The results showed that neither AG nor *B. megaterium* cells had a significant effect on the viability of exposed amebocytes. Therefore, we suggest that AG is able to inhibit the intracellular, inducible synthesis of NO from NOS during the immune response of earthworms.

The results from our NOS inhibition experiments are in close alignment with those of another study which also employed AG at the same concentration

Table 5 Average geometric mean of RFI values (± standard deviation) of NOS inhibition assays measured in FL-1 after overnight (13 - 16 h) incubation

		Baseline	SNAP	Bm only	Bm +AG (1000μM)	Bm + AG (250μM)
Assay A	EW 1	87.89 (±2.00)	141.02 (±7.00)**	90.19 (±2.06)	87.77 (±3.99)	88.05 (±1.31)
	EW 2	31.98 (±1.16)	73.89 (±0.52)***	38.88 (±0.89)*	34.17 (±0.43)*	36.89 (±0.38)*
	EW 3	47.46 (±0.47)	91.50 (±1.12)***	56.54 (±3.60)*	48.23 (±0.73)*	51.41 (±1.93)
	EW 4	32.14 (±1.32)	77.25 (±0.55)***	53.15 (±1.84)***	37.55 (±0.34)**	44.80 (±0.16)*
	EW 5	39.97 (±1.37)	69.42 (±1.56)**	42.70 (±1.60)*	39.35 (±0.95)*	40.79 (±0.91)*
	EW 6	56.87 (±2.85)	95.93 (±0.98)***	71.48 (±2.64)**	64.85 (±2.09)*	67.08 (±4.68)
Assay B	EW 7	33.99 (±0.53)	52.18 (±1.20)**	38.97 (±1.26)**	35.65 (±0.92)*	37.04 (±0.50)*
	EW 8	42.07 (±0.67)	60.79 (±1.17)**	43.81 (±1.32)	41.16 (±0.48)	43.88 (±0.25)
	EW 9	120.38 (±7.01)	217.81 (±2.90)**	134.31 (±4.24)	112.12 (±2.34)	125.78 (±4.13)
	EW 10	131.81 (±6.30)	198.74 (±12.71)*	152.97 (±1.10)*	140.52 (±2.78)*	153.13 (±2.80)
	EW 11	126.37 (±5.01)	208.94 (±7.16)**	144.14 (±7.90)**	124.59 (±4.67)	132.99 (±0.87)
	EW 12	26.99 (±0.59)	56.45 (±1.75)**	32.00 (±0.63)*	29.42 (±0.70)*	31.89 (±1.76)

The geometric mean of RFI corresponds to the concentration of NO present within each earthworm (EW) sample. Each sample was gated on R1 to include amebocytes only, excluding other cell populations. For each earthworm, the average geometric mean of RFI of the baseline negative control sample were compared to the average RFI of the positive control sample, SNAP and the RFI of immune-stimulated amebocyte samples exposed to *B. megaterium* (Bm) at a 200:1 MOI. Statistically significant NO levels above the baseline control are indicated with blue asterisks as: * = $p \leq 0.05$; ** = $p \leq 0.005$; and *** = $p \leq 0.0005$, as determined by student's t test: paired two samples for means. Also for each earthworm, the average RFI of immune-stimulated amebocyte samples exposed to *B. megaterium* (200:1 MOI) was compared to the average RFI of immune-stimulated amebocytes exposed to both *B. megaterium* (200:1) and aminoguanidine hydrochloride (AG) at a concentration of either 1000 μM or 250 μM. Statistically significant NO levels below the immune-stimulated control sample (Bm only) are indicated with red asterisks as: * = $p \leq 0.05$; ** = $p \leq 0.005$; and *** = $p \leq 0.0005$, as determined by student's t test: paired two samples for means.

(1,000 μM) to inhibit the inducible production of NO in celomocytes of the starfish *Asterias forbesi* following incubation with lipopolysaccharide (LPS) or PMA (Beck *et al.*, 2001). In the absence of AG, celomocyte stimulation by LPS or PMA resulted in significant increases in NO production, which was measured by the Griess method of nitrite quantification. When celomocytes were co-incubated with AG and the immunostimulant LPS or PMA, significant decreases in NO were observed. These results, in combination with those on NOS inhibition presented in the current study, suggest that invertebrate inducible NO is produced by the NOS enzyme during the innate immune response.

It is possible that the specificity of DAF-FM DA for NO may be affected by other derivatives such as superoxides, peroxyl radicals, or other DAF-reactive compounds. Limitations to using fluorescent probes for the detection of NO in living tissues have been reported (Uhlenhut and Högger, 2012). Because a decrease in fluorescence was observed when the NOS inhibitor aminoguanidine was included in the

Table 6 Amebocyte viability measurements following bacterial challenge with or without the addition of aminoguanidine

		Unlabeled Amebocytes	Unlabeled Amebocytes + Bm	Unlabeled Amebocytes + Bm + AG	Unlabeled Amebocytes + Saponin
Assay A	EW 1	87.31 (±0.64)	85.68 (±0.60)	86.24 (±1.29)	3.38 (±0.76)***
	EW 2	81.86 (±0.75)	78.57 (±1.02)	89.33 (±7.64)	25.39 (±1.99)*
	EW 3	89.97 (±1.28)	91.47 (±0.25)	90.76 (±0.70)	NT
	EW 4	87.87 (±0.52)	75.79 (±0.91)	76.45 (±0.13)	NT
	EW 5	93.37 (±1.12)	93.71 (±0.51)	94.18 (±0.11)	NT
	EW 6	81.22 (±1.39)	86.78 (±2.64)	83.46 (±0.55)	NT
Assay B	EW 7	89.08 (±1.10)	79.80 (±1.05)	80.02 (±0.72)	1.14 (±0.26)**
	EW 8	80.69 (±0.01)	79.31 (±2.47)	79.89 (±1.58)	23.85 (±0.38)**
	EW 9	76.57 (±0.02)	77.72 (±1.40)	77.39 (±1.80)	NT
	EW 10	74.87 (±2.10)	75.41 (±0.93)	75.47 (±0.42)	NT
	EW 11	90.80 (±0.35)	91.77 (±0.15)	91.10 (±0.37)	NT
	EW 12	94.56 (±0.60)	90.90 (±1.58)	91.97 (±0.98)	NT

Percentage of viable amebocytes in NOS inhibition assays are depicted. Viability was assessed by adding 7-AAD following the overnight (13 - 16 h) incubation period prior to flow cytometric analysis. Fluorescence was detected in FL-3; amoebocytes in earthworm (EW) samples that exhibited negative fluorescence were viable, while non-viable amebocytes exhibited positive fluorescence due to cellular uptake of 7-AAD. The detergent saponin was included in both assays in which two of the amebocyte samples per assay were exposed to facilitate the placement of quadrant markers to differentiate live from dead cells during data analysis. Statistically significant changes in viability compared to baseline control are indicated as: * = $p \leq 0.05$; ** = $p \leq 0.005$; and *** = $p \leq 0.0005$, as determined by student's t test: paired two samples for means. (NT = not tested).

assay, the data in this study support the claim that NO is induced by bacterial challenge, and that the increases in RFI observed can be attributed, at least in part, to a rise in NO production.

A high degree of variability of RFI values in baseline samples isolated from different earthworms between and within assays was observed in this study. A possible explanation for this variance is that the ratio of amebocytes to eleocytes is not consistent between individual earthworms as seen during cell enumeration on the hemacytometer and during data acquisition on the flow cytometer (data not shown). The rate of uptake of DAF-FM DA by amebocytes may have been influenced by the number of eleocytes in each sample. For example, the eleocytes may have a different affinity for the dye compared to the amebocytes which would affect the availability of the dye during extracellular uptake in the pre-labeling stage.

Through this laboratory investigation, we are able to gain a better understanding of the defense mechanisms utilized by invertebrates in response to microbial challenges that would be encountered naturally in their habitats. Going forward, we are interested in identifying more specifically which MAMPs are responsible for inducing NO production during the innate immune response. Also, due to the widespread inducible production of NO within both

invertebrates and vertebrates, further investigations on the conservation of the NOS gene throughout other phyla will help us to obtain more information on the functions of NO and their contribution to defense mechanisms. Other researchers recognize the significance of better understanding the role of NO, as the impact on the field of invertebrate ecological immunology could be great (Rivero, 2006). When assessing the role that the innate immune system plays in determining the fitness of organisms, the inducible production of NO could potentially serve as a survival advantage.

Acknowledgments

This work was funded by the Pennsylvania Academy of Science, the TriBeta Research Foundation, and the Cabrini College Science Department Research Fund.

References

Aderem A, Ulevitch RJ. Toll-like receptors in the induction of the innate immune response. Nature 406: 782-787, 2000.

Alderton WK, Cooper CE, Knowles RG. Nitric oxide synthases: structure, function and inhibition. Biochem. J. 357: 593-615, 2001.

Akman-Anderson A, Olivier M, Luckhart S. Induction of nitric oxide synthase and activation of signaling proteins in *Anopheles* mosquitos by the malaria pigment, hemozoin. Infect. Immun. 75: 4012-4019, 2007.

Bearoff FM, Fuller-Espie SL. Alteration of mitochondrial membrane potential ($\Delta\Psi m$) and phosphatidylserine translocation as early indicators of heavy metal-induced apoptosis in the earthworm *Eisenia hortensis.* Inv. Surv. J. 8: 98-108, 2011.

Beck G, Ellis T, Zhang H, Lin W, Beauregard K, Habicht GS, *et al.* Nitric oxide production by celomocytes of *Asterias forbesi*. Dev. Comp. Immunol. 25: 1-10, 2001.

Bogdan C. Nitric oxide and the immune response. Nat. Immunol. 2: 907-916, 2001.

Burgner D, Rockett K, Kwiatkowski D. Nitric oxide and infectious diseases. Arch. Dis. Child. 81: 185-188, 1999.

Choi SK, Choi HK, Kadono-Okuda K, Taniai K, Kato Y, Yamamoto M, *et al.* Occurrence of novel types of nitric oxide synthase in the silkworm, *Bombyx mori*. Biochem. Bioph. Res. Co. 207: 452-459, 1995.

Colasanti M, Venturini G. Nitric oxide in invertebrates. Mol. Neurobiol. 17: 157-174, 1998.

Conte A, Ottaviani E. Nitric oxide synthase activity in molluscan hemocytes. FEBS Lett. 365: 120-124, 1995.

Cooper E. Role of TOLL-like receptors in adjuvant–augmented immune therapies by T. Seya. Evid.-based Compl. Alt. 3: 133-137, 2006.

Cooper EL, Kauschke E, Cossarizza A. Digging for innate immunity since Darwin and Metchnikoff. Bioessays 24: 319-333, 2002.

Costa MM, Prado-Alvarez M, Gestal C, Roch P, Novoa B, Figueras A. Functional and molecular immune response of Mediterranean mussel (*Mytilus galloprovincialis*) haemocytes against pathogen-associated molecular patterns and bacteria. Fish Shellfish Immunol. 26: 515-523, 2009.

Dales RP, Kalaç Y. Phagocytic defense by the earthworm *Eisenia foetida* against certain pathogenic bacteria. Comp. Biochem. Physiol. 101A: 487-490, 1992.

Engelmann P, Molnár L, Pálinkás L, Cooper EL, Németh P. Earthworm leukocyte populations specifically harbor lysosomal enzymes that may respond to bacterial challenge. Cell Tissue Res. 316: 391-401, 2004.

Fuller-Espie SL. Vertebrate cytokines interleukin 12 and gamma interferon, but not interleukin 10, enhance phagocytosis in the annelid *Eisenia hortensis*. J. Invertebr. Pathol. 104: 119-124, 2010.

Fuller-Espie SL, Goodfield L, Hill K, Grant K, DeRogatis N. Conservation of cytokine-mediated responses in innate immunity: a flow cytometric study investigating the effects of human proinflammatory cytokines on phagocytosis in the earthworm *Eisenia hortensis*. Inv. Surv. J. 5: 124-134, 2008.

Fuller-Espie SL, Nacarelli T, Blake EL, Bearoff FM. The effect of oxidative stress on phagocytosis and apoptosis in the earthworm *Eisensia hortensis*. Inv. Surv. J. 7: 89-106, 2010.

Griffiths MJD, Messent M, MacAllister RJ, Evans TW. Aminoguanidine selectively inhibits inducible nitric oxide synthase. Br. J. Pharmacol. 110: 963-968, 1993.

Homa J, Zorska A, Wesolowski D, Chadzinska M. Dermal exposure to immunostimulants induces changes in activity and proliferation of celomocytes of *Eisenia andrei.* J. Comp. Physiol. B 183: 313-322, 2013.

Imamura M, Yang J, Yamakawa M. cDNA cloning, characterization and gene expression of nitric oxide synthase from the silkworm, *Bombyx mori.* Insect Mol. Biol. 11: 257-265, 2002.

Luckhart S, Rosenburg R. Gene structure and polymorphism of an invertebrate nitric oxide synthase gene. Gene 232: 25-34, 1999.

Luckhart S, Vodovotz Y, Cui L, Rosenberg R. The mosquito *Anopheles stephensi* limits malaria parasite development with inducible synthesis of nitric oxide. Natl. Acad. Sci. 95: 5700-5705, 1998.

Martínez A. Nitric oxide synthase in invertebrates. Histochem. J. 27: 770-776, 1995.

Nacarelli T, Fuller-Espie SL. Pathogen-associated molecular pattern-induced mitochondrial membrane depolarization in the earthworm *Eisenia hortensis*. J. Invertebr. Pathol. 108: 174-179, 2011.

Ottaviani E, Paeman LR, Cadet P, Stefano GB. Evidence for nitric oxide production and utilization as a bacteriocidal agent by invertebrate immunocytes. Eur. J. Pharmacol. 248: 319-324, 1993.

Rivero A. Nitric oxide: an antiparasitic molecule of invertebrates. Trends Parasitol. 22: 219-225, 2006.

Rodríguez-Ramos T, Carpio Y, Bolívar J, Espinosa G, Hernández-López J, Gollas-Galván T, *et al.* An inducible nitric oxide synthase (NOS) is

expressed in hemocytes of the spiny lobster *Panulirus argus*: Cloning, characterization and expression analysis. Fish Shellfish Immunol. 29: 469-479, 2010.

Škanta F, Roubalová R, Dvořák J, Procházková P, Bilej M. Molecular cloning and expression of TLR in the *Eisenia andrei* earthworm. Dev. Comp. Immunol. 41: 694-702, 2013.

Takeda K, Akira S. Roles of Toll-like receptors in innate immune responses. Genes Cells 6: 733-742, 2001.

Tenor JL, Aballay A. A conserved Toll-like receptor is required for *Caenorhabditis elegans* innate immunity. EMBO Rep. 9: 103-109, 2008.

Tumminello RA, Fuller-Espie SL. Heat stress induces ROS production and histone phosphorylation in celomocytes of *Eisenia hortensis*. Inv. Surv. J. 10: 50-57, 2013.

Uhlenhut K, Högger P. Pitfalls and limitations in using 4,5-diaminofluorescein for evaluating the influence of polyphenols on nitric oxide release from endothelial cells. Free Radic. Biol. Med. 52: 2266-2275, 2012.

Valembois P, Lasségues M. In vitro generation of reactive oxygen species by free celomic cells of the annelid *Eisenia fetida andrei:* an analysis by chemiluminescence and nitro blue tetrazolium reduction. Dev. Comp. Immunol. 19: 195-204, 1995.

Valembois P, Lasségues M, Roch P, Vaillier J. Scanning electron-microscopic study of the involvement of celomic cells in earthworm antibacterial defense. Cell Tissue Res. 240: 479-484, 1985.

Yeh F, Wu S, Lai C, Lee C. Demonstration of nitric oxide synthase activity in crustacean hemocytes and anti-microbial activity of hemocytes-derived nitric oxide. Comp. Biochem. Phys. B. 144: 11-17, 2006.